ESEEM and ENDOR Magnetic Resonance Studies of the Non-Kramers Doublet in the Integer-Spin Diiron(II) Forms of Two Methane Monooxygenase Hydroxylases and Hemerythrin Azide

Brian M. Hoffman,*,† Bradley E. Sturgeon,† Peter E. Doan,† Victoria J. DeRose,† Katherine E. Liu,‡ and Stephen J. Lippard*,‡

Departments of Chemistry, Northwestern University Evanston, Illinois 60208 Massachusetts Institute of Technology Cambridge, Massachusetts 02139

Received March 15, 1994

We report ESEEM and ENDOR[1,2] studies of the doubly-reduced, diiron(II) centers of the crystallographically characterized[3] methane monooxygenase hydroxylase ($MMOH_{red}$) from *Methylococcus capsulatus* (Bath), of the hydroxylase from *Methylococcus trichosporium* OB3b, and of hemerythrin azide (N_3Hr_{red}).[4] The diiron(II) state is pivotal in the catalytic cycle for methane oxidation by MMO and the respiratory function of hemerythrin because only this state reacts with dioxygen. In these diiron(II) centers the two ferrous ions are coupled by a ferromagnetic exchange interaction that is weak compared to the single-ion zero-field splitting (ZFS). The resulting integer-spin system exhibits a low-lying "non-Kramers" doublet that is split in zero applied field by an energy, Δ, the average value of which is in the microwave range, but which exhibits a spread in values.[5] The EPR properties of non-Kramers doublets have been well established for over 30 years,[6,7] and recently this knowledge has been applied to the study of metallobiomolecules such as $MMOH_{red}$ and N_3Hr_{red}.[8] To our knowledge, however, there are no prior reports of advanced magnetic resonance studies—ENDOR or ESEEM—on any non-Kramers doublet system.

Figure 1 presents representative three-pulse ESEEM[2] of N_3Hr_{red} and the two $MMOH_{red}$ taken in an X-band spectrometer with the microwave field (B_1) parallel to the applied field (B_0).[9] The echo amplitude is maximum at $B_0 = 0$ and decreases to ~0 by ~85 G for $MMOH_{red}$ and ~50 G for N_3Hr_{red}. Without an applied field none of the proteins shows significant nuclear modulation of the ESE envelope (e.g., Figure 1, $B_0 = 0$, N_3Hr_{red}). However, as B_0 is increased, modulation appears and Fourier transform of the time-domain traces[10] gives frequency spectra

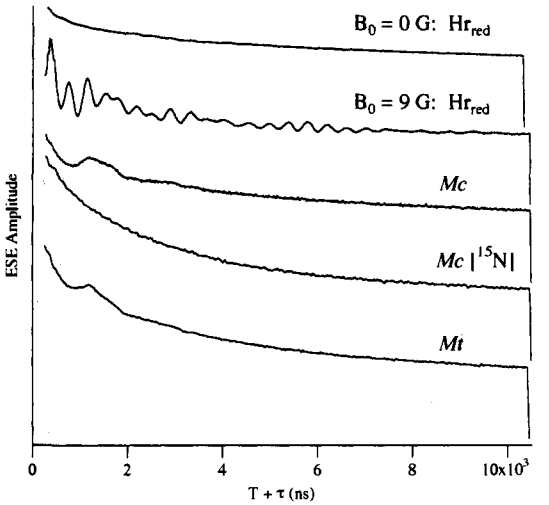

Figure 1. Representative normalized three-pulse ESEEM time domain spectra for N_3Hr_{red} and the *M. capsulatus* (*Mc*) and *M. trichosporium* (*Mt*) $MMOH_{red}$. Except for the top trace ($B_0 = 0$ G), all are at $B_0 = 9$ G, with $B_0 \| B_1$. Base lines are defined by the ending vertical lines. Conditions: approximately 5 W microwave power, 16-ns microwave pulse widths, 10-ms repetition time, 20-ns T steps, and temperature = 2 K. Other conditions: $\nu_e = 9.4$ GHz and τ (spacing between the first and second pulses) = 140 ns (N_3Hr_{red}), 160 ns ($MMOH_{red}$).

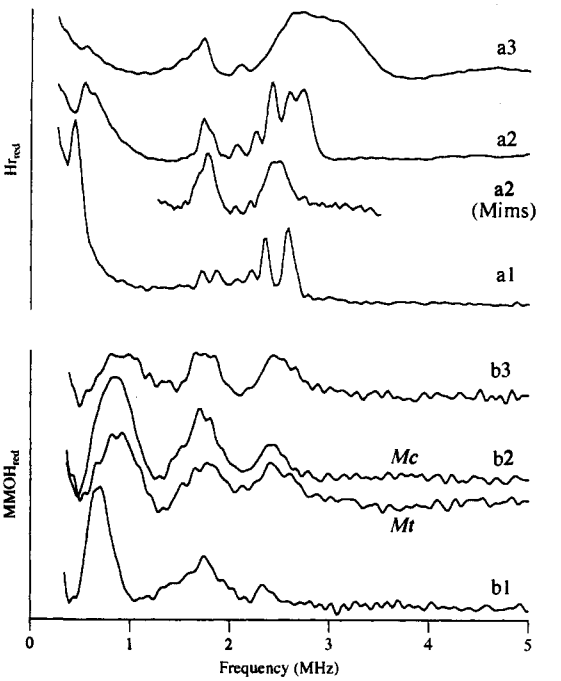

Figure 2. Three-pulse ESEEM frequency domain spectra for N_3Hr_{red} (a) and the *Mc* and *Mt* $MMOH_{red}$ (b). Field (B_0): a1 (×2), 1 G; a2, 9 G; a3, 27 G; b1 (×2), 9 G; b2, 16 G; b3 (×5), 20 G. Mims pulsed ENDOR (a2, $B_0 = 9$ G) is inset with a2. Conditions: For ESEEM, see Figure 1; for Mims ENDOR, $\nu_e = 9.433$, microwave power = 5 W, 16-ns microwave pulses, τ = 180 ns, 10-ms repetition time, 40-μs rf pulse, 200-W rf power, temperature = 2 K.

such as are presented in Figure 2. The spectra for N_3Hr_{red} show an array of sharp peaks; Mims pulsed ENDOR[2,11] measurements on N_3Hr_{red} generally match these spectra (Figure 2, a2). The patterns for the two $MMOH_{red}$ are virtually the same (e.g., Figure 2, b2), with three relatively broad lines. For both proteins the

† Northwestern University.

‡ Massachusetts Institute of Technology.

(1) Abbreviations: ENDOR, electron nuclear double resonance; ESEEM, electron spin echo envelope modulation; $MMOH_{red}$, reduced hydroxylase component of methane monooxygenase; N_3Hr_{red}, azidohemerythrin; ZFS, zero-field splitting.

(2) Berliner, L. J., Reuben, J., Eds.; *EMR of Paramagnetic Molecules*; Biological Magnetic Resonance 13; Plenum Press: New York, 1993.

(3) Rosenzweig, A. C.; Frederick, C. A.; Lippard, S. J.; Nordlund, P. *Nature* **1993**, *366*, 537–543.

(4) (a) Feig, A. L.; Lippard, S. J. *Chem. Rev.* **1994**, *94*, 759–805. (b) Que, L.; True, A. E. In *Progress in Inorganic Chemistry*; Lippard, S. J., Ed.; John Wiley & Sons: New York, 1990; Vol. 38, pp 201–258.

(5) Hendrich, M. P.; Münck, E.; Fox, B. G.; Lipscomb, J. D. *J. Am. Chem. Soc.* **1990**, *112*, 5861–5865.

(6) Tinkham, M. *Proc. R. Soc. London* **1956**, *A236*, 535–548.

(7) Griffith, J. S. *Phys. Rev.* **1963**, *132*, 316–319.

(8) Hendrich, M. P.; Debrunner, P. G. *Biophys. J.* **1989**, *56*, 489–506.

(9) (a) The pulsed spectrometer is described in the following: Fan, C.; Doan, P. E.; Davoust, C. E.; Hoffman, B. M. *J. Magn. Reson.* **1992**, *98*, 62–72. In these first experiments no effort was made to null the earth's field. (b) The protein preparation is described in the following: DeWitt, J. G.; Bentsen, J. G.; Rosenzweig, A. C.; Hedman, B.; Green, J.; Pilkington, S.; Papaefthymiou, G. C.; Dalton, H.; Hodgson, K. O.; Lippard, S. J. *J. Am. Chem. Soc.* **1991**, *113*, 9219–9235. Typical enzyme activities are 400–500 munits/mg and the Fe concentrations are usually ~2.5–3/MMOH following concentration. Similar values may be found in ref 5. [^{15}N]MMO was obtained by growing the *M. capsulatus* (Bath) organism on 99% enriched K[$^{15}NO_3$].

(10) Mims, W. B. *J. Magn. Reson.* **1984**, *59*, 291–306.

(11) Hoffman, B. M.; DeRose, V. J.; Doan, P. E.; Gurbiel, R. J.; Houseman, A. L. P.; Telser, J. In *EMR of Paramagnetic Molecules*; Biological Magnetic Resonance 13; Berliner, L. J., Reuben, J., Eds.; Plenum Press: New York, 1993; pp 151–218.

0002-7863/94/1516-6023$04.50/0 © 1994 American Chemical Society

peaks broaden and shift with increasing B_0, but the effect is larger for N_3Hr_{red}. In the case of $MMOH_{red}$ from *M. capsulatus*, ^{15}N substitution entirely abolishes the electron spin-echo modulation (Figure 1), proving that it arises solely from ^{14}N; the similarity between the results for the two $MMOH_{red}$ shows that the same must be true for the *M. trichosporium* enzyme. The spectrum for N_3Hr_{red} is analogous and is assigned similarly.

We interpret these observations as follows. The EPR transitions of the non-Kramers doublet state with hyperfine coupling to a nucleus of spin I can be described by eq 1, where ν_e (≈9.5 GHz) is the spectrometer frequency and θ is the angle between B_0 and an appropriate molecules axis.[6,7] Only the g and electron-nuclear

$$h\nu_e(m_I) = [\Delta^2 + (\tilde{g}_\parallel \beta B_0 \cos\theta + m_I \tilde{A}_\parallel)^2]^{1/2} \quad (1)$$

hyperfine tensor components parallel to the ZFS axis contribute, with $\tilde{g}_\parallel \approx (2M)g_e$ and $\tilde{A}_\parallel \approx (M)A_\parallel$ for a nonbridging atom ($A_\parallel$ is the single-ion hyperfine coupling), and $M = 4$ for a ferromagnetically coupled diiron(II) center. In a field-swept EPR spectrum eq 1 predicts the ordinary $2I + 1$ hyperfine lines separated by $\Delta B = \tilde{A}_\parallel/\tilde{g}_\parallel\beta$.[6] However, ESEEM and ENDOR measure energy separations within a nuclear manifold at fixed field.[11] For $\tilde{g}\beta B_z \ll \Delta$, as obtains here, we find[12] that these separations arise from an effective hyperfine coupling, A_{eff}, that depends linearly on B_z (eq 2). At the X band, A_{eff}(MHz) ~

$$A_{eff} = (\tilde{A}_\parallel \tilde{g}_\parallel \beta B_0 \cos\theta)/h\nu_e \quad (2)$$

$(A_\parallel(\text{MHz})\cos\theta)(B_0(\text{G})/100)$. As a result, the ENDOR frequencies for $I = {}^1/_2$ are linear in B_0.[12] For ^{14}N ($I = 1$) the nuclear Hamiltonian for the non-Kramers doublet includes the quadrupole interaction and an exact solution can be obtained[12] following Muha.[13] For clarity, however, we present the ENDOR frequencies for $I = 1$ correct to second order in the hyperfine interaction. Ignoring the nuclear-Zeeman contribution (insignificant at this low B_0), there are three transitions at frequencies ν_i ($i = +, -, 0$) that vary quadratically with B_0 (eq 3). The $\bar{\nu}_i$ are

$$\nu_i = \bar{\nu}_i + \sigma_i A_{eff}^2 \quad (3)$$

the three pure quadrupole frequencies, and the σ_i coefficients are easily derived.[12b] Because of the distribution in Δ, an ENDOR spectrum at a given B_0 exhibits the full range of frequencies predicted by eqs 2 and 3 because as $\cos\theta$ varies there is always a group of molecules with a Δ such that resonance occurs (eq 1).

As embodied in eqs 2 and 3, at zero field the electron and nuclear spins are uncoupled and there can be no echo modulation.[2] Application of a field establishes the coupling and introduces modulation.[14] Equation 3 predicts that, at low external fields, the spectrum for ^{14}N ($I = 1$) should tend toward the pure quadrupole pattern[16a] with three lines at $(\bar{\nu}_+, \bar{\nu}_-, \bar{\nu}_0)$, where $\bar{\nu}_0 + \bar{\nu}_- = \bar{\nu}_+$. The three lines for the two $MMOH_{red}$ in Figure 2 obey these conditions (e.g., Figure 2, b1: $\nu_0 = 0.65$ MHz, $\nu_- \sim 1.7$ MHz, $\nu_+ \sim 2.35$ MHz) and thus are provisionally assigned as such a set.[14b] The quadrupole tensor components corresponding to this assignment are $(P_x, P_y, P_z) = (1.0, 0.35, -1.35)$ MHz or, equivalently, $e^2qQ/h = 2.7$ MHz and $\eta = 0.48$.[16] The shifts with B_0 of the resonance frequencies for both N_3Hr_{red} and $MMOH_{red}$ (Figure 2) are consistent with the quadratic dependence of eq 3. The spectra are assigned to His ^{14}N directly bonded to ferrous iron;[16-18] the hyperfine coupling to the remote ^{14}N would be too low (~20-fold lower) to be responsible for the observed shifts (eqs 2, 3) or ESEEM modulation.[14] It is not possible to determine directly whether the pattern for $MMOH_{red}$ arises from coupling to one or both of the two coordinated His, but the crystal structure of the oxidized *M. capsulatus* hydroxylase[3] and ENDOR measurements on the mixed-valence state[17] lead us to suggest that it represents the unresolved signal from two similar His ^{14}N atoms. The equivalent spectroscopic signatures of the two MMOH proteins in the reduced state, as well as in the mixed-valence state,[17b] indicate that they have quite similar active-site structures. The additional peaks seen for N_3Hr_{red} require additional study, but must reflect differences among the ^{14}N His (five total) and azide ligands.[4]

In summary, in this first advanced magnetic resonance experiment on a non-Kramers system we have described the basis for spectral analysis, identified coupling to ^{14}N of His bound to the diiron(II) centers of $MMOH_{red}$ proteins from two different organisms, and discovered a related ^{14}N coupling for N_3Hr_{red}. Extensive studies are under way to explore other features of the diferrous state, which has hitherto been difficult to access spectroscopically.

Note Added in Proof: Experiments with $^{15}N_3Hr_{red}$ show that the high-frequency peak in Figure 2, a1 and doublet in a2, and the intensity above ~3 MHz in a3 are associated with ^{14}N of azide.

Acknowledgment. This work relied on the technical expertise of Mr. C. E. Davoust and was supported by the NIH (GM 32134 (S.J.L.); HL 13531 (B.M.H.); Predoctoral Trainee CA 09112 (K.E.L.); Postdoctoral GM 14259 (V.J.D.)) and the NSF (MCB 9207974 (B.M.H.)). We thank Dr. M. K. Bowman for helpful discussions and Prof. D. M. Kurtz, Jr. for Hr.

(12) (a) Hoffman, B. M. *J. Phys. Chem.*, submitted for publication. (b) For example, $\sigma_+ = (1/2)[\cos^2\alpha_2/\nu_+ + (\cos^2\alpha_3/\bar{\nu}_0 + \cos^2\alpha_1/\nu_-)/2]$ where the $\cos\alpha_i$ are the direction cosines of the ZFS z axis in the quadrupole frame; as an illustration, if all $\cos\alpha_i$ are equal, $\sigma_+ \approx \sigma_0 \approx 0.25$ MHz^{-1}; $\sigma_- \approx 0$.

(13) Muha, G. M. *J. Chem. Phys.* **1980**, *73*, 4139–4140.

(14) (a) Dr. M. K. Bowman has noted that echo modulation for a hyperfine-coupled $I = 1$ nucleus can occur *even* when the nuclear-Zeeman interaction is ignored. In this case the nuclear energies are identical in the two electron-spin manifolds *but* the wave functions are not. This introduces the state mixing required for ESEEM. (See ref 15.) (b) For $I = 1$, the modulation depth for each of the three transitions is proportional to the square of one of the $\cos\alpha_i$ in ref 12. Thus, not all transitions need appear for a given ^{14}N.

(15) Bowman, M. K.; Massoth, R. J. In *Electronic Magnetic Resonance of the Solid State*; Weil, J. A., Ed.; The Canadian Society for Chemistry: Ottawa, 1987; pp 99–110.

(16) According to eq 3 the $\bar{\nu}_i$ and thus the quadrupole couplings represent upper bounds. Refined values will be obtained through use of a simulation routine being developed. (a) Mims, W. B.; Peisach, J. In *Advanced EPR. Applications in Biology and Biochemistry*; Hoff, A. J., Ed.; Elsevier: Amsterdam, 1989; pp 1–57. (b) Bender, C.; Rosenzweig, A. C.; Lippard, S. J.; Peisach, J. *J. Biol. Chem.*; in press.

(17) (a) Hendrich, M. P.; Fox, B. G.; Andersson, K. K.; Debrunner, P. G.; Lipscomb, J. D. *J. Biol. Chem.* **1992**, *267*, 261–269. (b) DeRose, V. J.; Liu, K. E.; Lippard, S. J.; Hoffman, B. M. Manuscript in preparation.

(18) Gurbiel, R. J.; Batie, C. J.; Sivaraja, M.; True, A. E.; Fee, J. A.; Hoffman, B. M.; Ballou, D. P. *Biochemistry* **1989**, *28*, 4861–4871.